

## **Study on opening ventilation to reduce the wind load on a super tall building with recession corner**

\*Ting Deng<sup>1)</sup>, Ji-Yang Fu<sup>2)</sup>, Zhuang-Ning Xie<sup>3)</sup> and Yun-Cheng He<sup>4)</sup>

<sup>1),2),4)</sup> *Guangzhou University - Tamkang University Joint Research Center for Engineering Structure Disaster Prevention and Control, Guangzhou University, Guangzhou 510006, China*

<sup>3)</sup> *State Key Laboratory of Subtropical Building Science, South China University of Technology, Guangzhou, 510641, China*

<sup>1)</sup> [tdeng@gzhu.edu.cn](mailto:tdeng@gzhu.edu.cn)

### **ABSTRACT**

The wind pressures of super tall buildings with recession corner are tested in the wind tunnel by applying synchronous pressure measurement technology. The local aerodynamic measure (opening ventilation) is set at appropriate height. The results show that opening ventilation can significantly reduce the aerodynamic loads of structures. The maximum peak base bending moment corresponding to 100 year return period (YTP) and 50 YTP is reduced by 15.5% and 15.2% respectively. The peak acceleration corresponding to 10 YTP at top of building is reduced by 16%. Opening ventilation has less impact on the architectural shape, and is valuable to wind resistant design of super tall buildings.

### **1. INTRODUCTION**

Across-wind loads and responses are among the most significant factors determining the structural safety and comfort to the occupants of the super tall buildings in strong wind area. Aerodynamic shape plays an important role in controlling across-wind loads. Applying appropriate aerodynamic shape can reduce effectively the across-wind loads and responses of super tall buildings.

Merrick and Bitsuamlak (2009) examined the base loads of super tall buildings with five kinds of cross sections, namely, square, circle, triangle, rectangle and ellipse. It is found that the aerodynamic performance of a building with a triangle section was the best. Through a wind tunnel test of high-frequency force balance models, Yong et al. (2011) discussed the effects of the varying with height on wind-induced coupled motion of tall building with square cross-section. One basic conventional model, one

---

<sup>1)</sup> Assistant Professor

<sup>2)</sup> Professor

<sup>3)</sup> Professor

<sup>4)</sup> Associate Professor

setback model set back at the middle of the model height and two tapered models with taper ratios of 5% and 10% were used in this test. Results showed that the total rms acceleration response of setback and tapered models is smaller than that of the square model. Kim et al. (2002) investigated wind-induced response of models with 5%, 10%, and 15% tapering ratios and one basic model with a square cross-section by wind tunnel test, which were carried out under suburban and urban flow environments. It is founded tapering effect had a more significant effect in across-wind direction than that in along-wind direction and the tapering effect in suburban flow environment is more efficient than that of urban flow environment. Gu and Quan (2004) analyzed the wind-induced loads and responses of 15 typical high-rise buildings with various cross-sections. The effects of different aspect ratios, side ratios, and corner modifications on the base overturning moment were discussed in detail. They showed that corner modifications on buildings, such as chamfered and cut corners, could effectively suppress wind-induced responses. Tanaka et al. (2012) examined the aerodynamic forces and wind pressures acting on tall buildings with various unconventional configurations.

These research results above mostly focus on the varying of shape. However, the shape of super high-rise buildings is determined in the architectural design stage and it can't be varied for the structural designers. For this, this paper presents a new aerodynamic strategy to reduce the wind-induced loads and responses of super high-rise buildings. This new aerodynamic strategy is opening ventilation slots in the corner of equipment and refuge floors. The louvers are set at this location to keep the integrity of shape. It has almost no impact on the architectural features and function of super high-rise buildings. This new aerodynamic strategy is applied to a super high-rise building with round corner. Finally, the effect of opening ventilation slots on wind-induced loads and responses is discussed.

## **2. OUTLINE OF WIND TUNNEL EXPERIMENTS**

### *2.1 Configuration of building models*

Fig 1 presents the plan and elevation of the main tower. The height of the main tower with 56 floors above the ground is 248 meters. The architectural plane is obtained by processing the arcs in four corners of a square with a length of 45 meters and the whole structure is biaxial symmetry in plane arrangement and does not change from the bottom to the top section in the façade arrangement. There are only glass curtain above 238.5 meters height. The building has four equipment and refuge floors and its height is shown in Fig 1 (b).

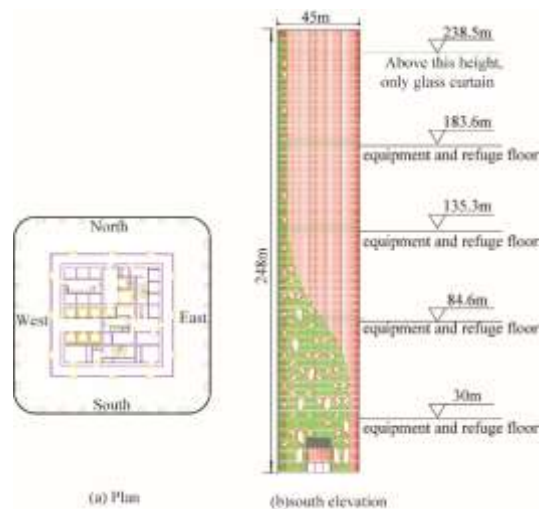


Fig 1 Plan and elevation of the main tower

## 2.2 Wind field simulation and experimental equipment

Wind tunnel tests were performed in the STDX-1 boundary layer wind tunnel at Shantou University. A test section of the wind tunnel with 3 m width, 2 m height, and 20 m length was utilized. Based on the surrounding terrain of studied building, according to the load code for the design of building structures in China (GB 50009-2001), B type of landform site is adopted and the coefficient of geomorphic roughness  $\alpha$  is equal to 0.16. The simulated profiles of mean wind speed and turbulence intensity in B type terrain are plotted in Fig. 2.

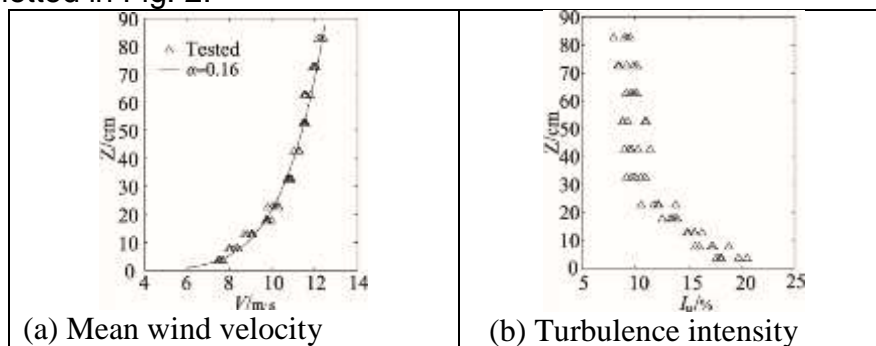


Fig. 2 Simulated wind parameters in wind tunnel

The pressure taps were installed in 9 levels of building model with various heights. There were 32 pressure taps on each level, and more taps were placed near the corner of the cross section to capture negative pressures characterized by flow separation on the side faces. The locations of the pressure taps that were denoted by the tap name and level number (A–H) are shown in Fig 3. L level and H level are the dual-side tap levels. The fluctuating wind pressure on the tap was recorded by a digital service module at a sampling frequency of 312.5 Hz. The sampling time was 65.536 s. The wind speed scale was set as 4.7. Thus, the sampling time in reality was 93 min according to the similarity law. The length of pressure tubing was set to a constant to minimize the influence of tubing response. All pressures were measured in reference to the undistributed ambient pressure in the wind tunnel as measured by the pitot- static

tube. Fig 4 shows the opening ventilation slot in the corner of equipment and refuge floors, so that wind can freely flow through it. The ventilation slots were 5.1 m in width; 5.1 m in length; and 3.8 m in height. Fig. 5 shows the models in the wind tunnel test.

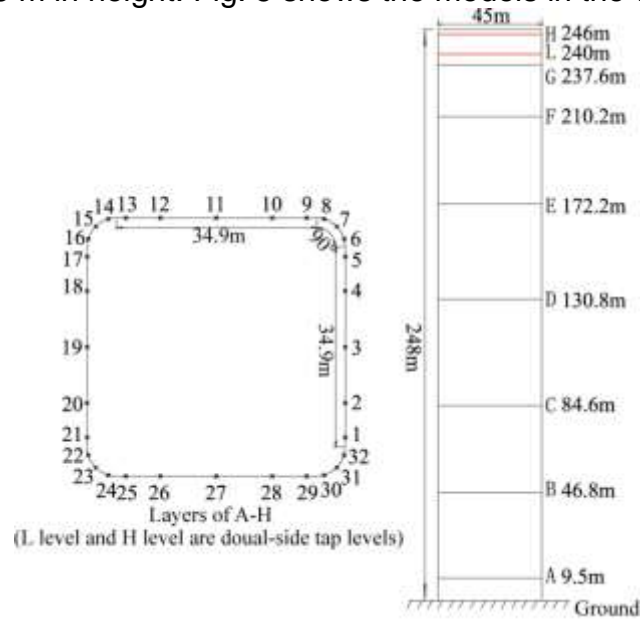


Fig 3. Pressure taps installed on model

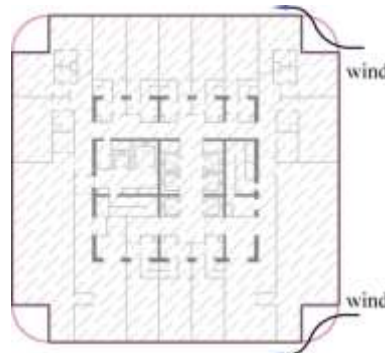


Fig 4. Schematic plan of opening ventilation slots



Fig. 5 Building model in wind tunnel

### 2.3 Data processing methods

The wind pressure time history  $p(t)$  of pressure tap can be obtained through wind tunnel tests; and the local aerodynamic loads at unit height is calculated by integration as follows:

$$F(t) = \int_L p(t) \cos \alpha_L dL \quad (1)$$

where  $L$  is the contour curve of buildings at the height of the pressure tap levels,  $\alpha_L$  is the angle between the contour curve and x or y axis. The base overturning moment is proportional to the first-order generalized force, when it is assumed that structural mode is linearly distributed along with the height of the building. Thus, the base overturning moment obtained from the integral of aerodynamic loads along with building height is an important indicator of aerodynamic performance. The aerodynamic overturning moment  $M_A$  can be represented as:

$$M_A = \int_0^H F(z) z dz \quad (2)$$

where  $F(z)$  is the local aerodynamic forces at the height  $z$ . Hence, the PSD of wind-induced base blending moment (BBM) can be further written as:

$$S_{M_D}(f) = |H(f)|^2 S_{M_A}(f) \quad (3)$$

where  $S_{M_A}(f)$  is the PSD of the base aerodynamic overturning moment  $M_A$  in Eq. (3).  $|H(f)|^2$  is the mechanical mobility of building, which can be obtained as:

$$|H(f)|^2 = \frac{1}{[1 - (f/f_0)^2]^2 + 4\zeta^2 (f/f_0)^2} \quad (4)$$

where  $\zeta$  is the modal damping ratio equal to 2.0% in the current study, and  $f_0$  is the first-order natural frequency equal to 0.098 Hz. Peak dynamic moment can be written as:

$$M_{D_{\max}} = \bar{M}_D + g\sigma_{M_D}, M_{D_{\min}} = \bar{M}_D - g\sigma_{M_D} \quad (5)$$

where  $\bar{M}_D$  is the mean moment,  $\sigma_{M_D}$  is the standard deviation of  $M_D$ , and  $g$  is the resonant peak factor. For a Gaussian process  $g = \sqrt{2\ln(f_0 T)} + 0.5772 / \sqrt{2\ln(f_0 T)}$  in which  $T$  is the observation time

### 3. Experimental results and discussions

In this paper, the local aerodynamic measure is employed to reduce aerodynamic loads on the studied structure. In order to make a convenient description, the scheme without considering aerodynamic measures is recognized as the original model. Above all, the aerodynamic load characteristics and peak response characteristics of the

original scheme are introduced. Based on the synchronous pressure test, equivalent static wind loads of the studied structure can be calculated by the extended load response correlation method. The maximum, minimum and average wind-induced loads including overturn-bending moments, torques and shear forces of the structural foundation can be obtained. The maximum, minimum, average of bending moments under the base loads around the X axis in 100a return period of the original model are shown in Fig. 6. It is indicated that the maximum value occurred at 0 and 180 degree wind direction. Because of the property of biaxial symmetry in the studied structure, the maximum base bending moments under the 0 and 180 degree wind directions are equal to  $-6.82 \text{ GN}\cdot\text{m}$  which exceed that under 90 and 270 degree wind directions. Meanwhile, the maximums of  $M_y$  under 90 and 270 degree wind directions are bigger than those under 0 and 180 degree wind directions, which indicates that the control wind direction is cross wind direction.

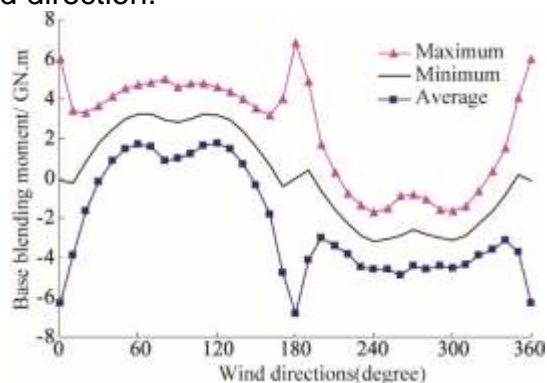


Fig 6 Base bending moment response vs. wind direction for case of original model

### 3.1 Effect on distribution of aerodynamic forces

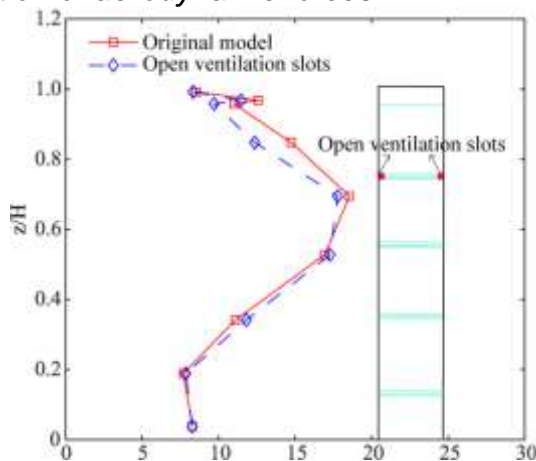


Fig 7 Variation of standard deviation of the local cross-wind aerodynamic force with height

Fig. 7 shows the effect of opening ventilation slots on the local cross-wind aerodynamic force with height. The maximum value occurs at the middle-top of building. Opening ventilation slot has less effect on the tap levels below itself height. It has more effect on the tap levels above itself height.

### 3.1 Effect on and wind-induced response

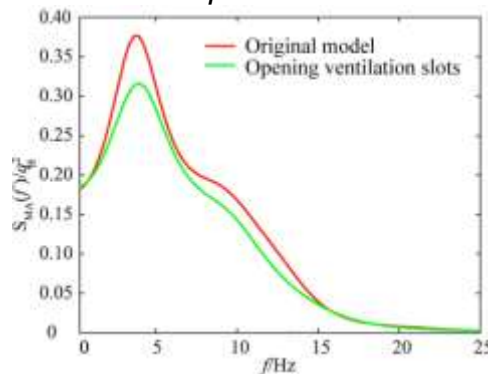


Fig 8 Comparison of PSD of base overturning moment

Table 1 Effective on reducing wind-induced dynamic building responses

Response	Return-period	Original model	Opening ventilation slots	Reduced effect
blending moment	100a	6.84GN · m	5.78 GN · m	15.5%
	50a	6.17 GN · m	5.23 GN · m	15.2%
acceleration	10a	17.7mg	14.6mg	16%

The comparison between power spectral density of the across-wind aerodynamic overturning moments is shown in Fig. 8. A peak related to vortex shedding occurs at about 4 Hz. Opening ventilation slots can decrease the value of power spectral densities of base aerodynamic moment at all frequency range. The nearer the initial natural frequency approximates to vortex shedding frequency, the better the mitigation effects are. Table 1 shows the mitigation effects of opening ventilation slots on peak dynamic moment at 100-year return period and 50-year return period, and peak acceleration at 10-year return period. The effects of opening ventilation slots on reducing wind-induced responses are significant.

### 3. CONCLUSIONS

The following conclusions can be obtained from this paper

- (1) Opening ventilation slots could significantly reduce the local cross-wind aerodynamic force above itself height.
- (2) The measure adopted in this paper could reduce the wind-induced loads of the building 100a and 50a recurrence period by 15.5% and 15.2% respectively.

### REFERENCES

- Gu, M. and Quan, Y. (2004), "Across-wind loads of typical tall buildings", *J. Wind Eng. Ind. Aerod.*, **92**(13), 1147-1165.

- Kim, Y.C., Kanda, J. and Tamura, Y. (2011), "Wind-induced coupled motion of tall buildings with varying square plan with height," *J. Wind Eng. Ind. Aerod.*, **99**(5), 638-650.
- Kim, Y.M. and You, K.P. (2002), "Dynamic response of a tapered tall building to wind loads", *J. Wind Eng. Ind. Aerod.*, **90**(12-15), 1771-1782.
- Merrick, R. and Bitsuamlak, G. (2009), "Shape effects on the wind-induced response of high-rise buildings," *J. Wind Eng.*, **6**(2), 1-18.
- Tanaka, H. and Tamura, Y., Ohtake, K., Nakai, M. and Kim, Y.C. (2012), "Experimental investigation of aerodynamic forces and wind pressures acting on tall buildings with various unconventional configurations", *J. Wind Eng. Ind. Aerod.*, 107-108, 179-191.